PRECIPITATION EXTREMES IN THE ARGENTINE PAMPAS: CURRENT DECLINING TRENDS AND PROJECTED INTENSIFICATION UNDER CLIMATE CHANGE

Andrea Soledad Brendel [1,2], Federico Ferrelli [1,3], Maria Cintia Piccolo [1,3]

[1] Instituto Argentino de Oceanografía (IADO-CONICET-UNS), Buenos Aires, Argentina
[2] Departamento de Agronomía, Universidad Nacional del Sur, Buenos Aires, Argentina
[3] Departamento de Geografía y Turismo, Universidad Nacional del Sur, Buenos Aires, Argentina

Manuscript received: September 15, 2025
Revised version: December 24, 2025

Brendel A S., Ferrelli F., Piccolo M C., 2026. Precipitation extremes in the Argentine Pampas: Current declining trends and projected intensification under climate change. *Quaestiones Geographicae* 45(3), Bogucki Wydawnictwo Naukowe, Poznań, pp. 51–67. 4 figs, 2 tables.

Abstract: Climate change is intensifying precipitation extremes globally, posing challenges to agriculture and water management in vulnerable regions such as the Argentine Pampas, one of the world's major agricultural zones. This study analyses long-term evolution of precipitation patterns and extremes in the Argentine Pampas to inform agricultural planning, water management and adaptation strategies. We examine spatiotemporal variability across three time periods: present (2010–2024), near future (2025–2039) and far future (2085–2099). Ten precipitation indices defined by the Expert Team on Climate Change Detection and Indices (ETCCDI) were assessed using data from 48 meteorological stations and projections from two global climate models (CCSM4 and CNRM-CM5) under RCP 4.5 and RCP 8.5 scenarios. Currently, several indices show significant decreasing trends, especially annual precipitation on wet days (Prcptot), where 71% of stations showed statistically significant trends (Mann–Kendall test, $p < 0.05$), maximum 1-day precipitation (RX1day) at 53% of decreasing stations, and consecutive wet days (CWD) at 73%. However, under the RCP 8.5 far-future scenario, rainfall extremes intensify substantially. Prcptot increases in 65% of stations (+160 mm/15 years), extremely wet days (R99p) increase in 88% of stations (+96 mm/15 years), and heavy precipitation days show marked increases in northern and eastern areas. The northeast emerges as the most vulnerable subregion, while southern and western areas show more moderate increases. These findings inform targeted adaptation strategies for managing future precipitation variability.

Keywords: extreme precipitation indices, climate projections, RCP scenarios, Mann–Kendall test, South America

Corresponding author: Andrea Soledad Brendel; asbrendel@iado-conicet.gob.ar

Introduction

Extreme meteorological events significantly impact society and the environment, with extreme precipitation being one of the primary triggers of natural disasters, including floods, landslides, soil erosion and crop destruction. Rainfall variability plays an essential role in water resource availability, which governs agriculture, river flow, hydroelectric power production, tourism and other economic activities crucial for economic and social development (de Melo-Goncalves et al. 2016). Global warming is intensifying the global hydrological cycle, altering precipitation patterns and increasing the probability and severity of extreme events in numerous regions

© 2026 Author(s)
This is an open access article distributed under the Creative Commons Attribution license

https://doi.org/10.14746/quageo-2026-0015
ISSN 2082-2103, eISSN 2081-6383

worldwide (IPCC 2021). Consequently, studies of spatiotemporal variations in precipitation and its extremes are becoming increasingly frequent (Li et al. 2020, Sun et al. 2021, dos Santos et al. 2024). In this context, precipitation has shown a positive trend across most of the planet since 1950, with an accelerated rate of increase since 1980 (IPCC 2021).

Recent regional studies have examined precipitation patterns across South America, providing essential context for understanding climate change impacts in the Pampean region. Medeiros et al. (2022) found that extreme precipitation events are expected to be more severe, frequent and long lasting in all Brazilian regions, while Ávila-Díaz et al. (2020) identified significant changes in precipitation patterns across different Brazilian regions using multiple reanalysis datasets and Earth System Model projections. These studies provide crucial background for understanding how global climate change manifests at the regional scale in the Pampas.

The IPCC Sixth Assessment Report (AR6) (IPCC 2021) indicates that by the end of the 21st century, under the high emission scenario SSP5-8.5, extreme precipitation could increase between 7% and 15% per degree of global warming, while under the low emission scenario SSP1-2.6, the increase would be between 4% and 8%. However, for this study, we utilise Representative Concentration Pathways (RCP) scenarios from the IPCC Fifth Assessment Report, as our climate model data were developed within the Coupled Model Intercomparison Project Phase 5 (CMIP5) framework. We use CMIP5-based models (CCSM4 and CNRM-CM5) based on their demonstrated highest regional validation performance for the Pampean region among 24 evaluated models (Rolla et al. 2018). Under RCP 8.5 (representing a high-emission pathway with continued fossil fuel dependence), extreme precipitation is projected to increase by approximately 7% per degree of global warming in many mid-latitude and wet tropical regions. In contrast, under the moderate mitigation scenario RCP 4.5, which assumes greenhouse gas (GHG) emissions peak around mid-century, followed by a gradual decrease, the intensification of extreme precipitation would be more contained. These findings underscore the need to understand the spatiotemporal variations of extreme rainfall to improve risk management and develop effective adaptation strategies (Donat et al. 2016, Bhatti et al. 2020).

The Pampean region (Argentina) is of high socioeconomic relevance due to its significant contribution to national and international agriculture. However, it is highly vulnerable to precipitation variations and extreme events, which have frequently led to drastic reductions in agricultural yields (Brendel et al. 2017), modified the water quality of its water resources (Paredes del Puerto et al. 2022), limited drinking water availability for the population (Casado, Campo 2019) and caused human and economic losses due to river flooding (Volonté, Gil 2019), among others.

Recent observational studies have documented significant changes in precipitation patterns across the Pampean region over the past several decades. Barros et al. (2015) identified increased precipitation trends in the eastern Pampas since the 1960s, while Aliaga et al. (2016) found enhanced precipitation variability and more frequent extreme events in the region since 1980. Additionally, Brendel et al. (2017) documented the increasing impact of precipitation extremes on agricultural yields, reflecting changes in both intensity and frequency of events. These observed changes provide important context for understanding projected future modifications in precipitation regimes under climate change scenarios. Therefore, it is fundamental to analyse the characteristics of extreme precipitation in this region, including its magnitude, frequency, and spatial distribution, to assess current and future risks associated with these events. This research aims to analyse trends and spatiotemporal variations of precipitation indices during the present and future in the Pampean region (Argentina). The results will provide key information for planning and developing adaptation strategies to address climate change impacts, as well as for protecting natural resources and ensuring the region's economic sustainability.

Study area

The Pampean region, located in the centre-east of the country, is Argentina's most important productive landscape, with an area of 721,353 km². Furthermore, this region represents approximately 75% of the cultivated area and

production of cereals and oilseeds in Argentina. Additionally, the agricultural sector contributes around 60% of Argentina's total exports (Ronco et al. 2016). Most of the region consists of extensive plains, although the altitude gradually increases from east to west (Fig. 1). The climate is temperate and humid, with precipitation decreasing in a northeast-southwest direction (1400–370 mm, Fig. 2), encompassing subtropical, arid, and semi-arid rainfall regimes (Aliaga et al. 2016). Dry and wet events are frequent and often affect water availability and human activities, primarily agriculture-related (Aliaga et al. 2016).

The precipitation regime in the Pampean region exhibits distinct seasonal patterns driven by multiple atmospheric systems. During summer, precipitation is primarily convective, associated with the South American Low-Level Jet that transports moisture from the Amazon basin and the South Atlantic Ocean (Reboita et al. 2019). Summer represents the wettest season in the northern and eastern areas, with frequent thunderstorms and intense precipitation events. Autumn represents a transitional period with decreasing precipitation totals, but persistent moderate events linked to frontal systems from the Pacific Ocean. Winter precipitation is dominated by extratropical cyclones and cold fronts, representing the driest season with lower intensity but events that are more persistent. Spring shows high variability, influenced by the interaction between subtropical and mid-latitude systems (Aliaga et al. 2016). The region's precipitation variability is differentially modulated by large-scale climate oscillations. The El Niño-Southern Oscillation (ENSO) primarily affects the northern and eastern portions of the Pampas, with El Niño events typically increasing precipitation while La Niña causes reductions (Cai et al. 2021). The southern and western sectors are more influenced

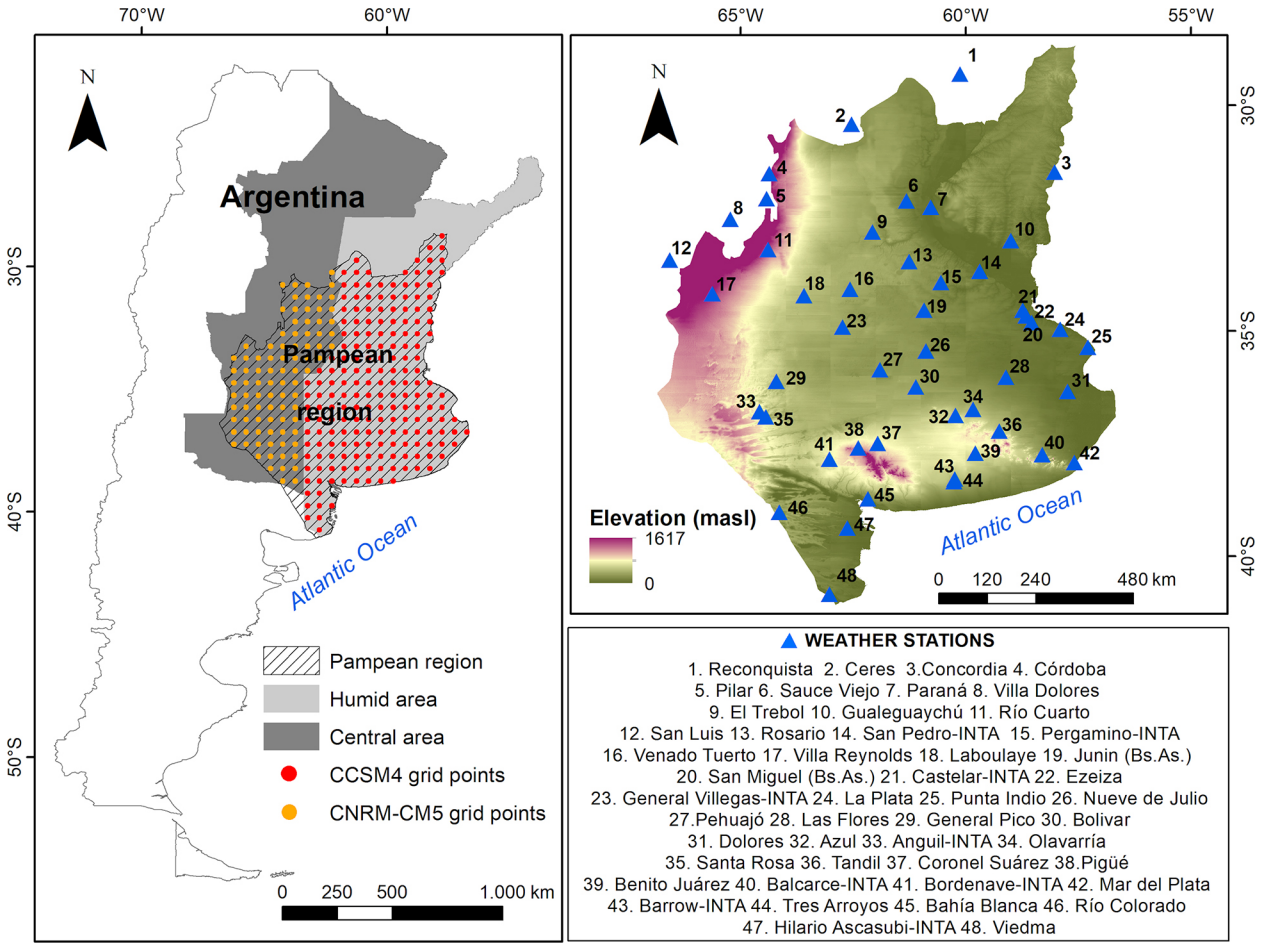


Fig. 1. Location of the Pampean region, Central and Humid areas and meteorological stations. Weather stations in close proximity due to map scale constraints are representing distinct locations with unique local climate variations.

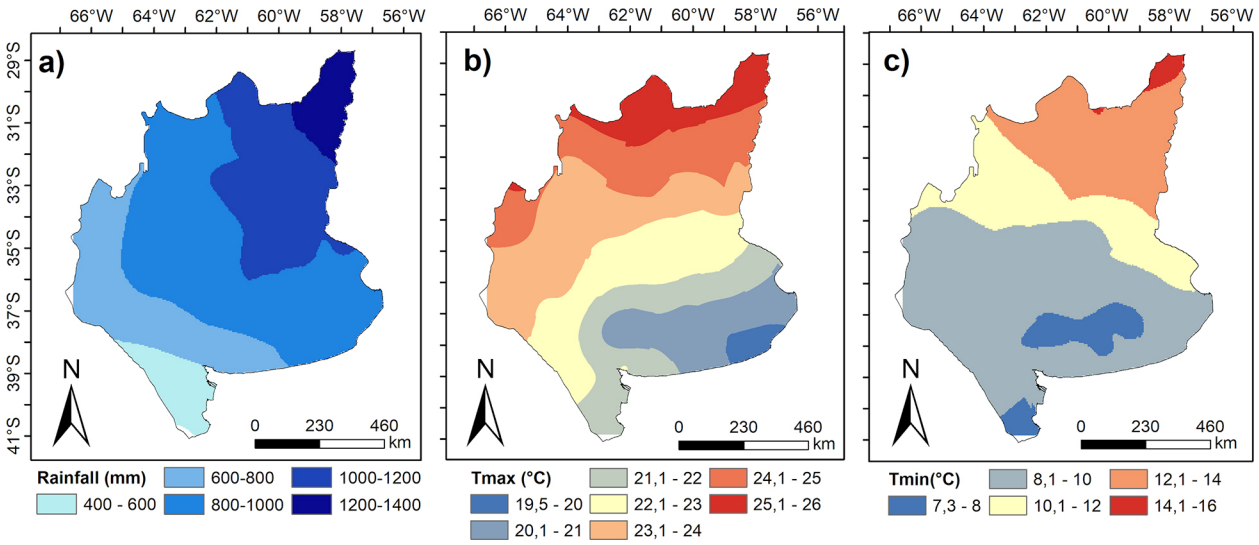


Fig. 2. A – mean annual precipitation (mm), B – mean annual maximum temperature (°C), and C mean annual minimum temperature (°C) in the Pampean region during the period 1960–2023.

by mid-latitude systems and show weaker ENSO teleconnections.

Extreme precipitation events in the current climate show regional differences: northern areas experience summer convective systems capable of producing intense daily totals, while southern regions are more affected by autumn-winter frontal systems generating sustained moderate-intensity precipitation over multiple days (National Meteorological Service, Argentina, 2023).

This area falls under the influence of the South Atlantic Convergence Zone (SACZ), a key component of the South American monsoon system that channels moisture from the Amazon basin south-eastward (Carvalho et al. 2011). Climate models project a strengthening and southward displacement of this system under warming scenarios (Zilli et al. 2019), which aligns with our findings of amplified precipitation extremes in the north-eastern Pampean region. These areas are more influenced by westerly mid-latitude systems and receive less moisture from tropical sources (Garreaud 2000).

The mean temperature ranges between 13 and 20°C, with a decreasing gradient from north to south. The Pampean region exhibits notable spatial variability in thermal characteristics. The mean annual maximum temperature (Fig. 2B) demonstrates a decreasing gradient from north to south, with the northern regions reaching 22.2–24.7°C and the southern regions ranging from 19.5 to 20.8°C. The mean annual minimum temperature (Fig. 2C) shows an inverse latitudinal trend, varying from 12.5–13.7°C in the northeast to 7.3–8.6°C in the southwest. This thermal distribution reflects the complex interplay of geographical factors, including latitude, continental influences, and proximity to the Atlantic Ocean.

Materials and methods

In situ data

Daily precipitation data from 48 meteorological stations located in the Pampean region were used during the period 2010–2024 (designated as present) (Fig. 1). The National Meteorological Service (SMN, Buenos Aires, Argentina) and the National Institute of Agricultural Technology (INTA, Buenos Aires, Argentina) provided the *in situ* data. A rigorous quality control process was implemented using R statistical software (R Core Team, Vienna, Austria) to ensure the quality and consistency of the meteorological data. Quality testing was performed using the RclimDex statistical package (ETCCDI, developed at Climate Research Division, Environment Canada, Toronto, Canada (Zhang, Yang 2004), while homogeneity assessment was conducted using the RHtests V4 package (Climate Research Division, Environment Canada, Toronto, Canada) (Wang et al. 2007). With these tools, the percentage of missing information and the number of outliers were calculated, which were <5% and 0.5%, respectively.

To address missing data, principal component analysis (PCA) was applied following the methodology detailed in Brendel et al. (2025). Daily precipitation data were pre-processed through square-root transformation, and the regularised iterative PCA algorithm was implemented using the R package 'missMDA'. Cross-validation optimisation yielded 7–9 principal components explaining 82–87% of variance, with validation showing root mean square errors below 2.5 mm for daily precipitation. This approach preserved the spatial and temporal covariance structure while maintaining statistical properties of the observed data, including extreme value distributions and spatial correlation structures across the study region.

A detailed station-by-station analysis revealed variability in missing data distribution across the network. While the overall average was <5%, individual stations showed heterogeneity in data completeness. Approximately 80% of stations had missing data rates below 4%, while six stations (13%) exhibited higher rates between 5% and 9%. For these stations with higher proportions of missing values, we implemented additional validation steps. First, we conducted a leave-one-out cross-validation procedure where a subset of known values was artificially removed and then reconstructed using our PCA approach. This validation revealed root mean square errors of <2.5 mm for daily precipitation, confirming the reliability of our gap-filling procedure even for stations with higher missing data percentages. Second, we performed sensitivity analyses by comparing regional trend results both with and without these stations, finding no significant differences in the identified spatial patterns or trend magnitudes. This multi-step validation process ensured that stations with variable missing data rates did not introduce systematic biases into our analysis, while maximising the spatial coverage of our observational network.

Modelled data

Daily rainfall data were downloaded from two global climate models obtained from the Centre for Marine and Atmospheric Research of Argentina (CIMA – 3cn.cima.fcen.uba.ar). The Community Climate System Model 4 (CCSM4 model), belonging to the National Centre for Atmospheric Research (NCAR, Boulder, United States), was used to characterise the Humid region (Fig. 1), while the Centre National de Recherches Météorologiques Coupled Models (CNRM-CM5 model) belonging to the National Centre for Meteorological Research (CNRM, Toulouse, France) was used to analyse the Central region (Fig. 1). While we acknowledge that using a larger ensemble of climate models would provide a more comprehensive representation of projection uncertainty, our selection was based on validated regional performance. These two models were specifically chosen because they demonstrated the highest skill in reproducing observed precipitation patterns in their respective subregions of the Pampas, as confirmed by previous validation studies (Rolla et al. 2018). This region-specific model selection approach allows us to reduce systematic biases in our projections while prioritising demonstrated accuracy over ensemble size.

Both models were developed as part of the CMIP5 that informed the IPCC Fifth Assessment Report. The CCSM4 model has a horizontal resolution of approximately 1.0° × 1.0° (longitude × latitude), equivalent to about 111 km × 111 km at the equator, while the CNRM-CM5 model has a resolution of 1.4° × 1.4° (approximately 155 km × 155 km). Both models were selected based on a validation study of 24 climate models conducted by CIMA as part of the baseline studies for the Third National Communication to the United Nations Framework Convention on Climate Change (Rolla et al. 2018).

These future time series were corrected using bias correction via quantile mapping to address systematic biases between modelled and observed data. This technique was implemented using the R package 'qmap', which compares the cumulative distribution functions (CDFs) of observed and modelled data during the reference period (2010–2024). The quantile-specific correction factors derived from this comparison were then applied to future projections, preserving the relative changes projected by the climate models while adjusting their absolute values to be consistent with historical observations. This approach has been demonstrated to effectively reduce systematic biases in climate model outputs while maintaining the climate change signal (Watanabe et al. 2012, Baimoung et al. 2014).

However, the quantile mapping bias correction method, although effective for systematic biases, assumes stationary relationships between observed and modeled quantiles that may not hold under climate change (Watanabe et al. 2012, Ferrelli et al. 2021). Additionally, analysing precipitation trends in relatively short periods (15 years) introduces additional uncertainties, as such timeframes may be strongly influenced by individual extreme events or interannual variability (Cristiano et al. 2017, Mahmood, Jia 2019). This limitation is particularly relevant for detecting trends in rare precipitation extremes, where a few intense events can disproportionately affect trend calculations (O'Gorman 2015).

The statistical quality of the models was evaluated by the CIMA using the Unified Model Validation Index (IUVM, from the Spanish *Índice Unificado de Validación de Modelos*), which ranges from 0 to 1. Values near zero correspond to poor fit, while those close to 1 indicate more accurate results. The IUVM is a composite index developed by CIMA to evaluate climate models' accuracy in reproducing regional climate patterns. This validation methodology integrates multiple statistical measures of agreement between modelled and observed climate data across Argentina. Specifically, the index evaluates:

1. spatial correlation patterns between simulated and observed temperature and precipitation fields,
2. model biases in representing mean climate conditions
3. accuracy in reproducing seasonal and annual cycles
4. skill in simulating climate extremes and
5. representation of interannual variability.

Each component is weighted according to its importance for regional climate processes, with greater emphasis placed on precipitation patterns for the Pampean region due to their critical role in agricultural productivity. The IUVM calculation involves normalising each statistical metric to a 0–1 scale and then computing a weighted average, resulting in a single comprehensive value that enables direct comparison between different climate models. This validation was conducted as part of the baseline studies for Argentina's Third National Communication to the United Nations Framework Convention on Climate Change. The CCSM4 model presented an IUVM value of 0.91, suggesting that, out of 24 models, it is the most accurate in representing future hydric and thermal conditions of the Humid region, while the CNRM-CM5 model was the most suitable for the Central region (Fig. 1), as its IUVM was also 0.90 (Rolla et al. 2018, Ferrelli et al. 2021). Therefore, these robust validation metrics provide substantial confidence in the reliability of both models, establishing a sound scientific foundation for employing them in climate projections and subsequent impact assessments within the Pampean region.

To enable direct comparison between observed station data and climate model outputs, we interpolated the model data to the precise geographical coordinates of each meteorological station. This spatial matching was performed using bilinear interpolation from the original model grid to the station locations. This approach preserves the large-scale patterns projected by the climate models while allowing point-based comparison with observations. For each station, we extracted the interpolated time series from either CCSM4 or CNRM-CM5 based on the station's geographical location (Humid or Central region, respectively). The interpolated model data maintained the temporal resolution of the original simulation (daily values) for consistent calculation of climate indices.

The future time series were analysed in two time periods. One was designated as near future (2025–2039) and the other as far future (2085–2099). Both time series were also obtained for two GHG concentration scenarios in the atmosphere (RCP). On the one hand, RCP 4.5 is a mitigation scenario in which GHG emissions stabilise by mid-century and gradually decrease (IPCC 2013). This scenario implies a significant reduction in fossil fuel dependence and an increase in the adoption of clean energy technologies and energy efficiency. On the other hand, RCP 8.5 represents a high-emission scenario where emissions continue to increase throughout the 21st century, with a constant and growing dependence on fossil fuels and the absence of effective mitigation policies (IPCC 2013).

Model integration and uncertainty analysis

To integrate the outputs from both models, we applied a spatial domain-specific approach.

The CCSM4 model outputs were used for the Humid region of the Pampas, while CNRM-CM5 outputs were used for the Central region, based on their respective validation scores. This approach was preferred over simple model averaging to preserve the higher-skill predictions of each model in its validated domain. The resulting analysis combines projections from both models while maintaining the regional advantages of each model's demonstrated performance in its respective area.

Calculation of climate indices

Ten climate indices defined by the Expert Team on Climate Change Detection and Indices (ETCCDI) (Peterson et al. 2001, Zhang et al. 2011) were analysed (Table 1). The calculation was performed using RClimDex software (Zhang, Yang 2004). These indices have been widely used to analyse the frequency, amplitude and persistence of daily extreme events in numerous regions worldwide (e.g., Chen et al. 2018, Zhou et al. 2018, Ferrelli et al. 2024). The indices were calculated using the previously described daily precipitation data and, as mentioned, were obtained for the present period (2010–2024), near future (2025–2039) and far future (2085–2099) under two GHG concentration scenarios (RCP 4.5 and RCP 8.5).

Statistical analysis of meteorological information

The trend of the 10 climate indices was calculated using the non-parametric Mann–Kendall test (Mann 1945, Kendall 1955) for the five study periods (present, near and far future under RCP 4.5 and RCP 8.5, respectively). The 10 climate indices were calculated on an annual basis for each meteorological station individually using daily precipitation data. For the indices that represent accumulated values (e.g., Prcptot, R95p, R99p), annual totals were computed for each year. For indices representing event frequency (e.g., R10, R20, R30), the total number of events per year was calculated. For indices representing maximum values (e.g., RX1day, RX5day) or maximum durations (consecutive dry days [CDD], consecutive wet days [CWD]), the maximum value for each year was determined. After obtaining these annual values for each station and each index, we calculated the trend for each of the five study periods (2010–2024, 2025–2039 under RCP 4.5, 2025–2039 under RCP 8.5, 2085–2099 under RCP 4.5, and 2085–2099 under RCP 8.5) using the Mann–Kendall test. This analysis was performed individually for each of the 48 meteorological stations, resulting in station-specific trends for each index and period. These station-level trends were then used to create the spatially interpolated maps shown in Figure 3, while the overall statistics of trend significance across stations were summarised in Table 2. Regional averages were calculated only after performing the station-level analyses, by averaging the Sen's slope values across all stations for each index and period, as reported in the 'Reg. Avg' column in Table 2.

This analysis was performed using R software with the Trend package (Pohlert 2017) in R Studio. The Mann–Kendall test, widely applied in climatological studies of thermal and hydrological trends (Shrestha et al. 2017, Brendel et

Table 1. Climate precipitation indices calculated in the present study.

Indices	Name	Definition	Units
Prcptot	Annual precipitation on wet days	Annual precipitation on wet days (pp > 1 mm)	$mm \cdot a^{-1}$
CDD	Consecutive dry days	Maximum number of consecutive days with pp < 1 mm	days
CWD	Consecutive wet days	Maximum number of consecutive days with pp > 1 mm	days
Rx1day	Maximum amount of precipitation occurred in 1 day	Wettest day of the year	mm
Rx5day	Maximum amount of precipitation occurred in 5 days	Five consecutive days with the highest precipitation	mm
R10	Days with heavy precipitation	Annual count of days when pp > 10 mm	days
R20	Days with very heavy precipitation	Annual count of days when pp > 20 mm	days
R30	Days with torrential precipitation	Annual count of days when pp > 30 mm	days
R95p	Very wet days	Amount of precipitation when pp > 95th percentile	mm
R99p	Extremely wet days	Amount of precipitation when pp > 99th percentile	mm

Table 2. Regional average rate of change and number of stations showing a significant decrease (D) or increase (I) in precipitation indices during five periods: present (2010–2024), near future (2025–2039), and far future (2085–2099), under RCP 4.5 and RCP 8.5 scenarios. 'RA' indicates the regional average rate of change over each 15 years, calculated using Sen's slope, not the actual precipitation values (presented as mean ± standard deviation across all 48 stations); 'N°' is the number of weather stations showing the directional change (positive or negative); and 'S' indicates the number of stations where these changes represent statistically significant trends according to the Mann–Kendall test with $p < 0.05$ as the significance threshold.

Indices	2010–2024					2025–2039 RCP 4.5					2085–2099 RCP 4.5					2025–2039 RCP 8.5					2085–2099 RCP 8.5				
	RA	D		I		RA	D		I		RA	D		I		RA	D		I		RA	D		I	
		N°	S	N°	S		N°	S	N°	S		N°	S	N°	S		N°	S	N°	S		N°	S	N°	S
Prcptot (mm)	−120 ± 91	28	20	20	5	63.2 ± 33.7	11	0	37	4	75.4 ± 52.5	22	2	26	7	11.9 ± 3.2	23	7	25	3	120.3 ± 50	17	0	31	26
RX1Day (mm)	−23.6 ± 4	30	16	18	2	13.7 ± 7	17	0	31	8	12.3 ± 5	15	0	33	2	13.4 ± 8	21	2	27	0	50.3 ± 15.1	19	0	29	18
RX5Day (mm)	−28.7 ± 14	30	14	18	2	20.7 ± 10	18	0	30	4	−14.6 ± 8	28	0	20	5	21.9 ± 7	23	0	25	0	37.4 ± 16	17	2	31	20
CWD (days)	−1 ± 0.7	26	19	22	9	1.4 ± 1.1	23	0	25	10	1.3 ± 0.7	23	6	25	2	1.5 ± 1.1	20	4	28	0	2.7 ± 0.7	13	3	35	26
CDD (days)	16 ± 11	17	3	31	19	9.5 ± 1.7	23	1	25	0	7.5 ± 3	14	2	34	4	−4.7 ± 1.1	28	4	20	1	−9.4 ± 1.9	35	24	13	6
R10 (days)	−3.9 ± 2	32	21	16	4	4.2 ± 2	13	0	35	4	3.9 ± 1.1	24	4	24	1	−4.3 ± 1.3	26	1	22	6	6.3 ± 1	18	3	30	29
R20 (days)	−4.3 ± 2	30	16	18	8	1.3 ± 1.2	19	2	29	1	−4.9 ± 1.9	30	3	18	4	−1.3 ± 0.9	25	2	23	1	6.9 ± 1	13	8	35	23
R30 (days)	1.6 ± 0.3	14	4	34	19	−2.1 ± 0.3	28	8	20	3	-1.6 ± 0.2	28	5	20	2	−2.5 ± 0.2	39	11	9	2	1.8 ± 0.2	11	2	37	26
R95p (mm)	−162.3 ± 30.2	27	17	21	9	−146.3 ± 40.3	29	5	19	3	−112.3 ± 16.8	29	11	19	5	−98.3 ± 23.1	38	8	10	1	190.3 ± 45.6	16	9	32	19
R99p (mm)	76.2 ± 19.3	10	2	38	19	79.4 ± 25.9	16	2	32	7	72.3 ± 18.5	17	3	31	5	−112.7 ± 13.1	39	5	9	2	83.1 ± 16.7	6	0	42	29

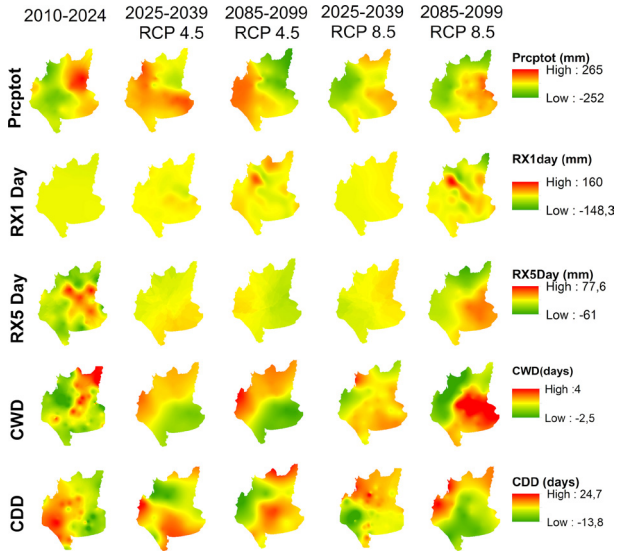


Fig. 3. Spatial trends in five precipitation climate indices (Prcptot, Rx1Day, Rx5Day, CWD and CDD) for present (2010–2024), near future (2025–2039) and far future (2085–2099) under RCP 4.5 and RCP 8.5 scenarios. Rate of change per 15 years using Sen's slope method. Red indicates increases, green indicates decreases. CDD, consecutive dry days; CWD, consecutive wet days; RCP, representative concentration pathways.

al. 2020, Ferrelli et al. 2024), assumes that under the null hypothesis (H_0: no monotonic trend exists in the series), the data are independent and identically distributed. When these assumptions are met, the test will not reject H_0 unless there is evidence of a true monotonic trend (increasing or decreasing, Ha). The Mann–Kendall test is measured using Kendall's Tau-b statistic. If this value is positive, then the series shows a positive trend; if the value is negative, the series has a negative trend. The trend is statistically significant if the p is <0.05. Additionally, to quantify the increase or decrease in thermal indices, Sen's estimator (Sen 1968) was applied. It is important to clarify the terminology used throughout this paper regarding changes in precipitation indices. We distinguish between:

1. 'Variations' or 'changes': These terms describe directional movements (positive or negative) in the values of indices over time, regardless of their statistical significance. These variations may be due to natural fluctuations or other factors and do not necessarily represent systematic changes.
2. 'Trends': This term is reserved exclusively for statistically significant directional chang-

es as confirmed by the Mann–Kendall test ($p < 0.05$). Only when the Mann–Kendall test indicates statistical significance do we consider that there is evidence of a systematic change or true trend in the data.

These results were interpolated in a Geographic Information System (ArcGIS 10.5, Esri, Redlands, United States) using ordinary spherical Kriging with a cell size of 0.01°. This technique assumes that the distance or direction between sample points has a spatial correlation that helps explain variation across an area (Menafoglio et al. 2013). Ordinary Kriging is one of the most widely used techniques in geostatistics and is highly suitable for representing climate data (Keskin et al. 2015, Aliaga et al. 2017, Ferrelli et al. 2019).

Results

The direction of changes and statistical significance of extreme rainfall indices across the five analysed periods are presented in Table 2, while Figures 3 and 4 illustrate their spatiotemporal variation. Notably, projections indicate that the most pronounced and statistically significant changes in the 10 analysed indices are found in the far future under the RCP 8.5 scenario, as evidenced by the statistical significance values presented in Table 2. Comparing variations across scenarios, we observed that changes under RCP 4.5 were generally less pronounced and showed limited statistical significance compared to RCP 8.5, particularly in the far future (Table 2). This pattern was consistent across most indices, suggesting that scenarios with lower GHG emissions (RCP 4.5) generally exhibited less pronounced changes in precipitation extremes compared to high-emission scenarios (RCP 8.5) in the Pampean region. However, even under this moderate emissions scenario, some variations toward increasing precipitation extremes were detected, albeit with lower magnitude and statistical confidence.

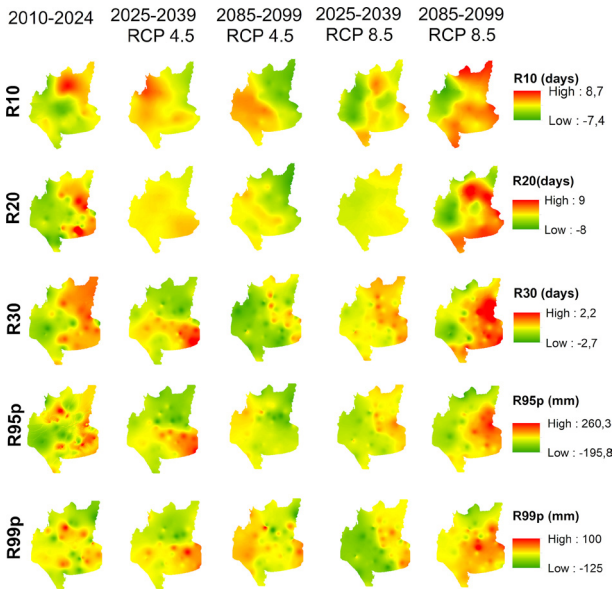


Fig. 4. Spatial trends in five extreme precipitation indices (R10, R20, R30, R95p and R99p) for present (2010–2024), near future (2025–2039) and far future (2085–2099) under RCP 4.5 and RCP 8.5 scenarios. Rate of change per 15 years using Sen's slope method. Warm colours indicate increases, cool colours indicate decreases. RCP, representative concentration pathway.

Based on these statistical considerations, our detailed analysis focuses on the far future RCP 8.5 scenario, where significant changes were robustly detected. Variations in annual precipitation on wet days (Prcptot) exhibited substantial variability, ranging between +265 mm and −252 mm across the five studied periods. During the present period, this index demonstrated a negative variation in 58% of the total 48 weather stations (28 stations), with 71% of these stations showing directional changes (20 out of 28) displaying statistically significant decreases. The regional average reduction amounted to −120 mm over 15 years (Fig. 3, Table 2). It is important to note that this regional average represents the central tendency calculated by averaging the Sen's slope values across all stations, while the range (+265 mm to −252 mm) reflects the maximum spatial variability observed at individual stations throughout the study region. This same principle applies to all precipitation indices discussed in this study, where regional averages (presented in Table 2) represent the central tendency across all stations, while the spatial patterns and extremes shown in Figures 3 and 4 illustrate the full range of variability across the Pampean region. This precipitation decline was predominantly concentrated in the central and western areas, while the eastern region exhibited non-significant increases.

In contrast, the far future scenario under RCP 8.5 revealed a marked shift, with 65% of stations (31 out of 48) showing positive variations.

Of these stations showing directional changes, 84% (26 out of 31) demonstrated statistically significant increases (Table 2). The spatial variation was particularly remarkable in the eastern region, where annual precipitation on wet days increased up to +160 mm/15 years. Additionally, the southern region exhibited a notable pattern reversal compared to the present period, with an increase of 45 mm over the 15-year analysis period (Fig. 3).

Maximum precipitation variations for 1-day (Rx1day) and 5-day (Rx5day) periods exhibited comparable statistics during the present study period, with negative trajectories observed in 63% of the 48 monitoring stations, and statistically significant trends found in 53% and 47% of the cases, respectively. Notably, both indices revealed a shift to positive trends during the far-future scenario under RCP 8.5. Specifically, RX1day demonstrated positive variations in 29 stations (60% of total), with the north-western region presenting the most pronounced maximum value of 160 mm/15 years. Likewise, RX5day exhibited increased precipitation in 31 stations (65% of the territorial coverage), but these are predominantly concentrated in the south-eastern part of the study area, while the southwestern region continues to show decreasing trends similar to the present period.

Variations in CWD and CDD exhibited contrasting spatial variations across the study period. During 2010–2024, CWD showed a negative variation, with a regional average reduction of −1 ± 0.7 days, statistically significant in 73% of stations showing directional changes (19 out of 26 stations) (Table 2). This decrease was most pronounced in the northwest, reaching −2.4 days over the 15 years (Fig. 3).

A notable pattern change emerged for the far future under the RCP 8.5 scenario, with CWD showing an average increase of 2.7 ± 0.7 days, statistically significant in 26 stations (74% of stations showing directional changes) (Table 2). This increase was particularly pronounced in the central and south-eastern regions, where CWD increments reached 4 days during the 15-year analysis period (Fig. 3). Concurrently, CDD exhibited a 65% positive trend, with an average increase of 16 ± 11 days and statistical significance in 62% of stations, predominantly concentrated in the central-south-western region (showing +16 days/15 years). The future projections under RCP 8.5 indicated a trend reversal, with an average reduction of −9.4 ± 1.9 days and statistical significance in 69% of stations (24 stations). This change was most pronounced in the central-south-eastern study area, demonstrating a reduction of 12 days over the 15 years (Fig. 3).

Rainfall intensity indices (R10, R20, and R30) exhibited significant spatial variations during the present study period, with percentages calculated both in relation to the total 48 stations and the variations observed. R10 and R20 demonstrated consistent spatial patterns, decreasing in 67% of the study region, which translates to 32 out of 48 stations for R10, and 30 out of 48 stations for R20, with >53% of these stations showing statistically significant trends according to the Mann–Kendall test (Table 2). For R10, during the present period (2010–2024), the most substantial reductions were observed in the western and southern territories, reaching −5.5 days per 15 years, while the northern region showed increases. Conversely, R20 showed the most pronounced decreases concentrated in the northwest and southwest regions, with reductions of −7 days per 15 years (Fig. 4).

In the far future scenario under RCP 8.5, a notable pattern reversal was projected. R10 increased in 63% of the region (30 out of 48 stations), with statistical significance in 97% of these stations showing increases (29 out of 30 stations). Similarly, R20 increased in 73% of the region (about 35 out of 48 stations), with statistical significance in 66% of these trend showing stations (23 out of 35 stations) (Table 2). The regional average increase approximated 6 days for both indices. Spatially, the most significant increase in R10 was evident in the northern region (reaching 8 days), while R20 demonstrated the most substantial increases in the north, south, and east, with increments up to 9 days during the 15-year analysis period (Fig. 4). R30 exhibited distinct behaviour, increasing during the present period in 71% of the study area (34 out of 48 stations), with statistical significance in 56% of these trend showing stations (roughly 19 out of 34 stations) (Table 2). This pattern not only continued but intensified in the far future under RCP 8.5, affecting 77% of the region (37 out of 48 stations), with notable increases of up to 2 days/15 years concentrated towards the eastern region (Fig. 4).

Extreme precipitation indices R95p and R99p exhibited contrasting variations during the present study period (Table 2). R95p decreased in 56% of the territory, which corresponds to 27 out of 48 stations, with the most substantial reductions concentrated in the central and western regions, reaching up to −136 mm. Conversely, R99p demonstrated positive trends in 79.1% of the area (38 out of 48 stations), with substantial increases of up to 89 mm in the north and select central sectors (Fig. 4).

In the future scenario under RCP 8.5, both indices revealed a significant shift towards positive trends. R95p increased in 67% of the region (32 out of 48 stations), while R99p showed an even more pronounced increase, affecting 88% of the area (42 out of 48 stations). The spatial pattern of these trends was more distinctly defined compared to the present period. The northeast and central-eastern regions experienced the most substantial increases: R95p reached +214 mm/15 years, and R99p increased by +96 mm/15 years. In contrast, the southern region exhibited more moderate increases, with R95p showing +42 mm/15 years and R99p registering +64 mm/15 years (Fig. 4). Statistical significance varied between the two indices, with R99p demonstrating more consistent trends. Approximately 59% of weather stations (roughly 28 out of 48 stations) showed statistically significant trends for R99p, indicating a more robust pattern of extreme precipitation changes (Table 2).

Integrating the results of the 10 analysed indices, a coherent pattern of climate change emerges in the Pampean region. The current directional change toward drier conditions (evidenced by decreases in Prcptot, CWD, R10 and R20) is projected to reverse by the end of the 21st century, particularly under the RCP 8.5 scenario. This reversal will not be uniform in either spatial distribution or precipitation characteristics. While the eastern region will experience increases in both frequency and intensity of precipitation, the western region will primarily show an increase in intensity with less pronounced changes in frequency. This differentiated pattern reflects the interaction between regional atmospheric mechanisms and global warming, where the enhanced moisture-holding capacity of the atmosphere manifests heterogeneously based on pre-existing geographical and climatic characteristics.

Discussion

Changes in global and regional precipitation characteristics are one of the most relevant aspects of climate change in a warming world. However, there is little consensus on observed and expected rainfall changes (Donat et al. 2016). Pampas represents one of the world's leading agricultural production centres, contributing significantly to global food security (FAO 2023). With production representing approximately 12% of the international grain trade and 40% of Argentine agricultural production (Bert et al. 2021), its productive stability is crucial for global agricultural markets. This region is susceptible to variations in precipitation patterns since >80% of its production depends on rainfed agriculture (Barros et al. 2015). Changes in precipitation patterns directly affect agricultural yields and the entire agro-industrial value chain (Brendel et al. 2017).

This study presents, for the first time, a comprehensive analysis of extreme rainfall events in Pampas (Argentina) that combines:

1. the joint analysis of 10 precipitation indices,
2. a high density of weather stations covering the entire region and
3. the connection between present variations and future projections under different climate change scenarios.

While previous studies have analysed specific aspects such as rainfall regimes (Aliaga et al. 2016), isolated dry and wet events (Aliaga et al. 2017), particular impacts on agriculture (Brendel et al. 2017), or water resources characteristics (Casado, Campo 2019), this work provides a complete spatial and temporal characterisation of rainfall and its future changes.

Scientific interpretation of spatial and temporal precipitation patterns

The observed reversal in precipitation patterns between the present and future periods represents a notable finding that requires scientific interpretation. This non-linear response indicates that the current drying directional change in the region may not represent a continuous trajectory but rather a transitional state in a shifting climate regime. Similar non-linear climate responses have been documented in other South American regions, where precipitation regimes

show decadal-scale oscillations superimposed on longer-term climate change signals (Grimm, Tedeschi 2009). The Pampa region specifically has historically exhibited multi-decadal precipitation cycles linked to basin-scale oceanic oscillations (Kayano, Capistrano 2014), but our findings suggest that anthropogenic warming may fundamentally alter these natural cycles.

The strong spatial heterogeneity in projected precipitation changes reveals important insights about regional atmospheric dynamics. The pronounced intensification of extreme events in the north-eastern Pampas likely reflects the interaction between increasing atmospheric moisture capacity and regionally specific circulation patterns. The more moderate increases projected for southern and western regions can be explained by their position relative to large-scale circulation patterns. The differential response to warming between these distinct atmospheric influences creates the intensified northeast-southwest precipitation gradient projected under future scenarios. This scientific interpretation goes beyond describing spatial variability to explaining its underlying causes in atmospheric dynamics.

Temporally, the stark contrast between current decreasing trends and projected future increases indicates a potential threshold response in the regional hydroclimate system. Such non-linear temporal responses can emerge when opposing factors influencing precipitation reach tipping points (Boers et al. 2017). In the current period, factors favouring drying conditions (potentially including land-use changes, natural variability cycles, or aerosol effects) may temporarily outweigh GHG warming effects. However, as warming intensifies under high emission scenarios, the thermodynamic enhancement of the hydrological cycle appears to overwhelm these opposing influences, particularly for extreme precipitation events where the Clausius-Clapeyron scaling becomes more directly relevant (O'Gorman 2015).

Our focus on RCP 8.5 for detailed spatial analysis is supported by previous studies that have found similar limitations in statistical significance under moderate emissions scenarios. Pinto et al. (2018) found that precipitation extremes under RCP 4.5 showed weaker signals compared to RCP 8.5 across multiple regions globally, while Chen and Sun (2018) reported that RCP 4.5 projections rarely achieved statistical significance before mid-century. This pattern of statistical robustness under higher versus moderate emission scenarios provides additional context for interpreting the spatial patterns identified in our analysis.

Model limitations and uncertainty analysis

Despite the robustness of our findings, several methodological limitations should be acknowledged. First, while our selection of two climate models (CCSM4 and CNRM-CM5) was based on their validated regional performance, a larger ensemble would provide a more comprehensive representation of projection uncertainty. As highlighted by studies on climate model evaluation (IPCC 2013, Bauer et al. 2015), precipitation remains one of the most challenging variables for climate models to simulate accurately due to the complex microphysical processes involved and the high spatial variability of precipitation events. The differences observed between our two models, particularly in precipitation frequency indices (CWD, CDD) and in western regions, reflect these inherent simulation challenges.

Second, the quantile mapping bias correction method, although effective for systematic biases, assumes stationary relationships between observed and modelled quantiles that may not hold under climate change (Watanabe et al. 2012, Ferrelli et al. 2021). Third, the limitations of bias correction methods in non-stationary climates (as discussed in Methods) may introduce additional uncertainties in trend detection. Additionally, a more comprehensive uncertainty assessment focusing on forecast reliability and ensemble spread would strengthen future projections in this region. Nevertheless, our approach of combining high-density observations with domain-validated models and robust statistical testing provides a solid foundation for understanding precipitation extremes in the Pampean region under climate change.

Implications for regional management and adaptation

These projected changes in rainfall patterns will have significant implications for various sectors of the Pampean region. Therefore, the early implementation of adaptation measures would

not only reduce future costs but could also create opportunities for developing resilient and sustainable systems (IPCC 2013, Sloat et al. 2020). These changes could affect regional and global food security, given the crucial role of Pampas in international agricultural production (Ferrelli et al. 2019). In the farming sector, the increase in the intensity of extreme events, particularly in the east and north of the region, could increase the risks of soil erosion and crop loss (Brendel et al. 2017, Zhang et al. 2019). Water management systems will need to adapt to greater variability in precipitation, especially in areas where the largest increases in extreme events are projected (R95p and R99p). Increasing precipitation intensity could overwhelm existing infrastructure, mainly urban and rural drainage systems (Volonté, Gil 2019).

This spatial heterogeneity in projected changes suggests the need to develop specific adaptation strategies for each subregion, considering both local characteristics and the expected magnitude of changes in different extreme precipitation indices (Di Bella et al. 2017, Seneviratne et al. 2021). In the eastern and north-eastern areas, where a higher frequency of extreme events is projected, it will be crucial to strengthen early warning systems and improve drainage infrastructure to manage larger precipitation volumes (Di Bella et al. 2017, Volonté, Gil 2019). In the agricultural sector, these areas might require adopting more conservative soil management practices and selecting crops more resistant to excess water conditions (Scarpati, Capriolo 2018).

On the other hand, although the western and southern subregions show more moderate increases, they will also need to adapt their production and water management systems to handle greater projected variability in extreme precipitation events. This situation is particularly critical in the southern Pampean region, where high rates of water and wind erosion already exist and where more intense precipitation events could exacerbate existing erosive processes, compromising the sustainability of production systems (Bouza et al. 2012, Ferrelli 2017). Furthermore, urban planning and infrastructure development must incorporate these new climate scenarios into their designs. Sustainable urban drainage systems, water retention areas and the implementation of green infrastructure could be key strategies to increase city resilience against more intense precipitation events (Perillo et al. 2023). Additionally, continuous monitoring of these changes will be fundamental to adjust and improve adaptation strategies as projected impacts develop, as various authors have pointed out (Zhang et al. 2019, Seneviratne et al. 2021).

Future research directions

Building on the findings and limitations of this study, several key directions for future research emerge. First, expanding the analysis to include a larger ensemble of climate models would provide a more comprehensive representation of projection uncertainty and strengthen confidence in the identified patterns. Multi-model ensembles can better characterise the range of possible future precipitation changes and provide probabilistic projections that are more useful for risk-based decision-making (Tebaldi, Knutti 2007).

Second, exploring the interactions between precipitation changes and other climate variables, particularly temperature and evapotranspiration, would provide a more complete picture of future hydroclimate changes. The compound effects of changing precipitation patterns and rising temperatures could have synergistic impacts on agricultural systems, water resources, and natural ecosystems beyond what either factor would produce independently (Seneviratne et al. 2010). Third, integrating precipitation projections with hydrological modelling would help translate atmospheric changes into impacts on streamflow, soil moisture, groundwater recharge and flood risk. Such integrated assessments are essential for developing effective adaptation strategies, particularly for water resource management and flood control infrastructure (Hirabayashi et al. 2013).

Added value of precipitation extreme analysis and compound climate risks

This precipitation-focused analysis provides critical insights that cannot be obtained through temperature-only studies, particularly for understanding compound climate risks in agricultural systems. As highlighted by Zscheischler et al. (2020), compound events involving multiple climate variables often produce impacts that

exceed those of individual extremes, making a separate analysis of precipitation and temperature essential for comprehensive risk assessment. Precipitation extremes drive fundamentally different impact pathways compared to temperature extremes: while temperature affects physiological crop stress and growing season length, precipitation governs soil moisture dynamics, flood-drought cycles, and erosion processes that determine long-term land productivity (Seneviratne et al. 2021).

Our findings of intensifying precipitation extremes in eastern Pampas, combined with the warming trends documented in Brendel et al. (2025), reveal emerging risks of heat-wetness compounds that could trigger crop diseases, soil waterlogging and harvest disruptions. Conversely, the moderate precipitation increases in western regions, coupled with rising temperatures, suggest heightened heat-drought compound risks similar to those affecting other mid-latitude agricultural regions (Ojima et al. 2021). These compound interactions exhibit non-linear impacts on agricultural yields that cannot be predicted from single-variable analyses (Donat et al. 2016). This precipitation extreme analysis thus complements our temperature study by providing the hydrological foundation necessary for comprehensive climate risk assessment, enabling the development of location-specific adaptation strategies that address the full spectrum of compound climate hazards facing agricultural systems (Ford et al. 2011, Seneviratne et al. 2021).

Conclusion

This study provides the first comprehensive assessment of current and future changes in extreme rainfall events in the Pampean region. Using two climate models (CCSM4 and CNRM-CM5) selected for their regional performance, we analysed different timeframes and scenarios, focusing primarily on the far-future under RCP 8.5 where projections showed statistical significance. Our results reveal a clear reversal in precipitation patterns between the present and future periods. Currently, several indices exhibit statistically significant decreasing trends – especially Prcptot (71% of decreasing stations), RX1day (53%), and CWD (73%). This contrasts sharply with projected intensification under RCP 8.5, where annual precipitation increases in 65% of stations (+160 mm/15 years), extremely wet days (R99p) increase in 88% of stations (+96 mm/15 years) and heavy precipitation days show marked increases in northern and eastern areas.

The northeast emerges as the most vulnerable subregion to extreme precipitation changes, while southern and western areas show more moderate increases. CWD are projected to increase by 2.7 ± 0.7 days, while CDD decreases by 9.4 ± 1.9 days, indicating a fundamental shift in precipitation patterns across the entire region.

Each model was applied to its respective region based on validation performance, with CCSM4 used for the humid region and CNRM-CM5 for the central region. While this approach leverages each model's regional strengths, we acknowledge limitations, including the use of different models for different subregions and 15-year analysis periods. Despite these constraints, our findings provide valuable insights for identifying regional vulnerabilities and developing targeted adaptation strategies.

Our multi-index approach advances methodological frameworks for detecting climate change signals in precipitation extremes, showing that different indices reveal complementary aspects of changing precipitation regimes. The results provide crucial information for improving water resource management and developing climate-resilient infrastructure in one of the world's main agricultural regions, while recognising the need for locally tailored implementation strategies that account for inherent uncertainties in precipitation projections.

Acknowledgements

We thank the National Meteorological Service (SMN, Argentina), the National Institute of Agricultural Technology (INTA, Argentina), and the Centre for Marine and Atmospheric Research (CIMA, Argentina) for providing data. We also thank two anonymous reviewers for their valuable comments that made this article better.

Funding

This research was funded by the National Scientific and Technical Research Council

(CONICET) and the Universidad Nacional del Sur (UNS) through grants PICT-2021-I-INVI-00580 and PIBAA28720210100943CO.

Authors' contributions

A.S.B.: Conceptualisation, Data collection, Writing Original Draft, Project administration, Investigation, Data analysis, Visualisation, Writing, Review and Editing. F.F.: Methodology, Data analysis, Writing Review and Editing, Supervision. M.C.P.: Writing, Review and Editing, Supervision. All authors have read and agreed to the published version of the manuscript.

References

Aliaga V.S., Ferrelli F., Alberdi-Algarañaz E., Bohn V.Y., Piccolo M.C., 2016. Distribution and variability of precipitation in the Pampas, Argentina. *Cuadernos de Investigación Geográfica* 42(1): 261–280. DOI 10.18172/cig.2867.

Aliaga V.S., Ferrelli F., Piccolo M.C., 2017. Regionalization of climate over the Argentine Pampas. *International Journal of Climatology* 37(S1): 1019–1035. DOI 10.1002/joc.5079.

Ávila-Díaz A., Benezoli V., Justino F., Torres R., Wilson A., 2020. Assessing current and future trends of climate extremes across Brazil based on reanalyses and earth system model projections. *Climate Dynamics* 55: 1403–1426. DOI 10.1007/s00382-020-05333-z.

Baimoung S., Oki T., Archevarahuprok B., Yuttaphan A., Pangpom M., 2014. Bias correction techniques for meteorological data of A2 scenario climate model output in Chao Phraya River Basin of Thailand. *Hydrological Research Letters* 8: 71–76. DOI 10.3178/hrl.8.71.

Barros V.R., Boninsegna J.A., Camilloni I.A., Chidiak M., Magrín G.O., Rusticucci M., 2015. Climate change in Argentina: Trends, projections, impacts and adaptation. *Wiley Interdisciplinary Reviews: Climate Change* 6(2): 151–169. DOI 10.1002/wcc.316.

Bauer P., Thorpe A., Brunet G., 2015. The quiet revolution of numerical weather prediction. *Nature* 525(7567): 47–55. DOI 10.1038/nature14956.

Bert F., de Estrada M., Naumann G., 2021. The 2017-18 drought in the Argentine Pampas – Impacts on agriculture. GAR special report on drought. United Nations Office for Disaster Risk Reduction, , Geneva, Switzerland.

Bhatti A.S., Wang G., Ullah W., Ullah S., Fiifi Tawia Hagan D., Kwesi Nooni I., Ullah I., 2020. Trend in extreme precipitation indices based on long term *in situ* precipitation records over Pakistan. *Water* 12(3): 797. DOI 10.3390/w12030797.

Boers N., Marwan N., Barbosa H.M., Kurths J., 2017. A deforestation-induced tipping point for the South American monsoon system. *Scientific Reports* 7(1): 41489. DOI 10.1038/srep41489.

Bouza M.E., Silenzi J.C., Echeverría N.E., De Lucia M.P., 2012. Analysis of erosive events for a soil in the southwest of Buenos Aires Province, Argentina. *Aeolian Research* 3(4): 427–435. DOI 10.1016/j.aeolia.2011.10.001.

Brendel A.S., Bohn V.Y., Piccolo M.C., 2017. Variabilidad de la precipitación y su relación con los rendimientos agrícolas en una región semiárida de la llanura pampeana (Argentina). *Estudios Geográficos* 78: 7–29. DOI 10.3989/estgeogr.201701.

Brendel A.S., del Barrio R.A., Mora F., León E.A.O., Flores J.R., Campoy J.A., 2020. Current agro-climatic potential of Patagonia shaped by thermal and hydric patterns. *Theoretical and Applied Climatology* 142: 855–868. DOI 10.1007/s00704-020-03350-w.

Brendel A.S., Ferrelli F., Piccolo M.C., 2025. Temperature extremes and warming trends in the Argentine Pampas: Present patterns and future projections under climate change. *Environmental Earth Sciences* 84: 123–145. DOI 10.1007/s12665-025-10234-5.

Cai W., Santoso A., Collins M., Dewitte B., Karamperidou C., Kug J.S., Lengaigne M., McPhaden M.J., Stuecker M.F., Taschetto A.S., Timmermann A., Wu L., Yeh S.W., Wang G., Ng B., Jia F., Yang Y., Ying J., Zheng X.T., Bayr T., Brown J.R., Capotondi A., Cobb K.M., Gan B., Geng T., Ham Y.G., Jin F.F., Jo H.S., Li X., Lin X., McGregor S., Park J.H., Stein K., Yang K., Zhang L., Zhong W., 2021. Changing El Niño–Southern Oscillation in a warming climate. *Nature Reviews Earth and Environment* 2: 628–644. DOI 10.1038/s43017-021-00199-z.

Carvalho L.M., Jones C., Silva A.E., Liebmann B., Silva Dias P.L., 2011. The South American monsoon system and the 1970s climate transition. *International Journal of Climatology* 31(8): 1248–1256. DOI 10.1002/joc.2147.

Casado A., Campo A.M., 2019. Extremos hidroclimáticos y recursos hídricos: estado de conocimiento en el suroeste bonaerense, Argentina. *Cuadernos de Geografía* 28(2): 43–66. DOI 10.30827/cuadgeo.v58i1.6751.

Chen A., He X., Guan H., 2018. Trends and periodicity of daily temperature and precipitation extremes during 1960-2013 in Hunan Province, Central South China. *Theoretical and Applied Climatology* 132: 71–88. DOI 10.1007/s00704-017-2069-x.

Chen H., Sun J., 2018. Projected changes in climate extremes in China in a 1.5°C warmer world. *International Journal of Climatology* 38(9): 3607–3617. DOI 10.1002/joc.552.

Cristiano E., Ten Veldhuis M.C., van de Giesen N., 2017. Spatial and temporal variability of rainfall and their effects on hydrological response in urban areas – A review. *Hydrology and Earth System Sciences* 21: 3859–3878. DOI 10.5194/hess-21-3859-2017.

de Melo-Goncalves P., Rocha A., Santos J.A., 2016. Robust inferences on climate change patterns of precipitation extremes in the Iberian Peninsula. *Physics and Chemistry of the Earth, Parts A/B/C* 94: 114–126. DOI 10.1016/j.pce.2016.05.003.

Di Bella C.M., Paruelo J.M., Becerra J.E., Bacour C., Baret F., 2017. Effect of senescent leaves on NDVI-based estimates of fAPAR: Experimental and modelling evidences. *International Journal of Remote Sensing* 38(20): 5632–5650. DOI 10.1080/01431160412331269724.

Donat M.G., Lowry A.L., Alexander L.V., O'Gorman P.A., Maher N., 2016. More extreme precipitation in the world's dry and wet regions. *Nature Climate Change* 6(5): 508–513. DOI 10.1038/nclimate2941.

dos Santos A.L.M., Gonçalves W.A., Andrade L.D.M.B., Rodrigues D.T., Batista F.F., Lima G.C., e Silva C.M.S., 2024. Space-time characterization of extreme precipitation indices for the semiarid region of Brazil. *Climate* 12(3): 43. DOI 10.3390/cli12030043.

FAO., 2023. The state of food security and nutrition in the world 2023. FAO, IFAD, UNICEF, WFP and WHO, Rome.

Ferrelli F., 2017. Variabilidad pluviométrica y sus efectos sobre las coberturas del suelo al sur de la provincia de Buenos Aires, Argentina. *Revista Geográfica Venezolana* 58(1): 26–37.

Ferrelli F., Brendel A.S., Aliaga V.S., Piccolo M.C., Perillo G.M.E., 2019. Climate regionalization and trends based on daily temperature and precipitation extremes in the south of the Pampas (Argentina). *Cuadernos de Investigación Geográfica* 45(1): 393–416. DOI 10.18172/cig.3707.

Ferrelli F., Brendel A.S., Perillo G.M.E., Piccolo M.C., 2021. Warming signals emerging from the analysis of daily changes in extreme temperature events over Pampas (Argentina). *Environmental Earth Sciences* 80(12): 422. DOI 10.1007/s12665-021-09721-4.

Ferrelli F., Pontrelli Albisetti M., Brendel A.S., Casoni A.I., Hesp P.A., 2024. Appraisal of daily temperature and rainfall events in the context of global warming in South Australia. *Water* 16(2): 351. DOI 10.3390/w16020351.

Ford J.D., Berrang-Ford L., Paterson J., 2011. A systematic review of observed climate change adaptation in developed nations. *Climatic Change* 106(2): 327–336. DOI 10.1007/s10584-011-0045-5.

Garreaud R., 2000. Cold air incursions over subtropical South America: Mean structure and dynamics. *Monthly Weather Review* 128(7): 2544–2559. DOI 10.1175/1520-0493(2000)128<2544:CAIOSS>2.0.CO;2.

Grimm A.M., Tedeschi R.G., 2009. ENSO and extreme rainfall events in South America. *Journal of Climate* 22: 5206–5219. DOI 10.1175/2008JCLI2429.1.

Hirabayashi Y., Mahendran R., Koirala S., Konoshima L., Yamazaki D., Watanabe S., Kim H., Kanae S., 2013. Global flood risk under climate change. *Nature Climate Change* 3(9): 816–821. DOI 10.1038/nclimate1911.

IPCC., 2013. Chapter 12: Climate Change 2013: The physical science basis. In: Stocker T.F., Qin D., Plattner G.K., Tignor M., Allen S.K., Boschung J., Nauels A., Xia Y., Bex V., Midgley P.M. (eds), *Contribution of Working Group I to the Fifth Assessment Report of the Intergovernmental Panel on Climate Change*. Cambridge University Press, Cambridge, United Kingdom and New York, NY, USA: 1029–1136.

IPCC., 2021. Climate Change 2021: The Physical Science Basis. In: Masson-Delmotte V., Zhai P., Pirani A., Connors S.L., Péan C., Berger S., Caud N., Chen Y., Goldfarb L., Gomis M.I., Huang M., Leitzell K., Lonnoy E., Matthews J.B.R., Maycock T.K., Waterfield T., Yelekçi O., Yu R., Zhou B. (eds), Contribution of Working Group I to the Sixth Assessment Report of the Intergovernmental Panel on Climate Change. Cambridge University Press, Cambridge, United Kingdom and New York, NY, USA.

Kayano M.T., Capistrano V.B., 2014. How the Atlantic Multidecadal Oscillation (AMO) modifies the ENSO influence on the South American rainfall. *International Journal of Climatology* 34(1): 162–178. DOI 10.1002/joc.3674.

Kendall M.R., 1955. *Rank correlation methods*, 4th Edn. Charles Griffin, London.

Keskin M., Dogru A.O., Balcik F.B., 2015. Comparing spatial interpolation methods for mapping meteorological data in Turkey. In: Energy Systems and Management. Springer, Cham, Switzerland, pp. 33–42. DOI 10.1007/978-3-319-16024-5_3.

Li L., Zou Y., Li Y., Lin H., Liu D.L., Wang B., Song S., 2020. Trends, change points and spatial variability in extreme precipitation events from 1961 to 2017 in China. *Hydrology Research* 51(3): 484–504. DOI 10.2166/nh.2020.095.

Mahmood R., Jia S., 2019. Analysis of climate variability, trends, and prediction in the most active parts of the Lake Chad Basin, Africa. *Scientific Reports* 9: 6317. DOI 10.1038/s41598-019-42811-9.

Mann H.B., 1945. Non-parametric tests against trend. *Econometrica: Journal of the Econometric Society* 13: 245–259. DOI 10.2307/1907187.

Medeiros F.J., Oliveira C.P., Avila-Diaz A., 2022. Evaluation of extreme precipitation climate indices and their projected changes for Brazil: From CMIP3 to CMIP6. *Weather and Climate Extremes* 38: 100511. DOI 10.1016/j.wace.2022.100511.

Menafoglio A., Secchi P., Dalla Rosa M., 2013. A universal kriging predictor for spatially dependent functional data of a Hilbert space. *Electronic Journal of Statistics* 7: 2209–2240. DOI 10.1002/9781119387916.ch2.

O'Gorman P.A., 2015. Precipitation extremes under climate change. *Current Climate Change Reports* 1(2): 49–59. DOI 10.1007/s40641-015-0009-3.

Ojima D.S., Conant R.T., Parton W.J., Lackett J.M., Even T.L., 2021. Recent climate changes across the Great Plains and implications for natural resource management practices. *Rangeland Ecology and Management* 78: 180–190. DOI 10.1016/j.rama.2021.03.008.

Paredes del Puerto J.M., García I.D., Maiztegui T., Paracampo A.H., Rodrigues Capitulo L., Garcia de Souza J.R., Colautti D.C., 2022. Impacts of land use and hydrological alterations on water quality and fish assemblage structure in headwater Pampean streams (Argentina). *Aquatic Sciences* 84(1): 6. DOI 10.1007/s00027-021-00842-3.

Perillo V.L., Brendel A.S., Ferrelli F., Gutiérrez A., Vitale A.J., Marinangeli P., Piccolo M.C., 2023. CO2 flux dynamics of exotic and native species in an extensive green roof simulator with hydric deficit. *Urban Climate* 49: 101567. DOI 10.1016/j.uclim.2023.101567.

Peterson T.C., Folland C., Gruza G., Hogg W., Mokssit A., Plummer N., 2001. *Report on the activities of the working group on climate change detection and related rapporteurs 1998–2001*. World Meteorological Organization, Geneva, Switzerland.

Pinto I., Jack C., Hewitson B., 2018. Process-based model evaluation and projections over southern Africa from coordinated regional climate downscaling experiment and coupled model intercomparison project phase 5 models. *International Journal of Climatology* 38(11): 4251–4261. DOI 10.1002/joc.5666.

Pohlert T., 2017. Trend: Non-parametric trend tests and change-point detection. R package version 1.1.0. Online: CRAN.R-project.org/package=trend (accessed December 12, 2025).

Reboita M.S., Ambrizzi T., Silva B.A., Pinheiro R.F., da Rocha R.P., 2019. The South Atlantic Subtropical Anticyclone: Present and future climate. *Frontiers in Earth Science* 7: 8. DOI 10.3389/feart.2019.00008.

Rolla A.L., Nuñez M.N., Guevara E.R., Meira S.G., Rodriguez G.R., Ortiz de Zárate M.I., 2018. Climate impacts on crop yields in Central Argentina. Adaptation strategies. *Agricultural Systems* 160: 44–59. DOI 10.1016/j.agsy.2017.08.007.

Ronco A.E., Marino D.J.G., Abelando M., Almada P., Apartin C.D., 2016. Water quality of the main tributaries of the Paraná Basin: Glyphosate and AMPA in surface water

and bottom sediments. *Environmental Monitoring and Assessment* 188: 458. DOI 10.1007/s10661-016-5467-0.

Scarpati O.E., Capriolo A.D., 2018. Evolución del exceso de agua edáfica anual en la Región Pampeana (Argentina) Evolution of annual soil water surplus in Pampean Region (Argentina). *Estudios Geográficos* 79(285): 375–395. DOI 10.3989/estgeogr.201814.

Sen P.K., 1968. Estimates of the regression coefficient based on Kendall's tau. *Journal of the American Statistical Association* 63: 1379–1389. DOI 10.1080/01621459.1968.10480934.

Seneviratne S.I., Corti T., Davin E.L., Hirschi M., Jaeger E.B., Lehner I., Orlowsky B., Teuling A.J., 2010. Investigating soil moisture–climate interactions in a changing climate: A review. *Earth-Science Reviews* 99(3–4): 125–161. DOI 10.1016/j.earscirev.2010.02.004.

Seneviratne S.I., Zhang X., Adnan M., Badi W., Dereczynski C., Di Luca A., Ghosh S., Iskandar I., Kossin J., Lewis S., 2021. Chapter 11: Weather and climate extreme events in a changing climate. In: Masson-Delmotte V., Zhai P., Pirani A., Connors S.L., Péan C., Berger S., Caud N., Chen Y., Goldfarb L., Gomis M.I., Huang M., Leitzell K., Lonnoy E., Matthews J.B.R., Maycock T.K., Waterfield T., Yelekçi O., Yu R., Zhou B. (Eds.), Climate Change 2021: The physical science basis. Contribution of Working Group I to the Sixth Assessment Report of the Intergovernmental Panel on Climate Change. Cambridge University Press, Cambridge, UK.

Shrestha N.K., Du X., Wang J., 2017. Assessing climate change impacts on fresh water resources of the Athabasca River Basin, Canada. *Science of the Total Environment* 601: 425–440. DOI 10.1016/j.scitotenv.2017.05.013.

Sloat L.L., Davis S.J., Gerber J.S., Moore F.C., Ray D.K., West P.C., Mueller N.D., 2020. Climate adaptation by crop migration. *Nature Communications* 11(1): 1–9. DOI 10.1038/s41467-020-15076-4.

SMN (National Meteorological Service), Argentina, 2023. Climatological statistics. Servicio Meteorológico Nacional, Buenos Aires. Online: smn.gob.ar (accessed December 12, 2025).

Sun Q., Zhang X., Zwiers F., Westra S., Alexander L.V., 2021. A global, continental, and regional analysis of changes in extreme precipitation. *Journal of Climate* 34(1): 243–258. DOI 10.1175/JCLI-D-19-0892.1.

Tebaldi C., Knutti R., 2007. The use of the multi-model ensemble in probabilistic climate projections. *Philosophical Transactions. Series A, Mathematical, Physical, and Engineering Sciences* 365: 2053–2075. DOI 10.1098/rsta.2007.2076.

Volonté A., Gil V., 2019. Aportes de la hidrogeomorfología histórica en la determinación de áreas inundables a partir de eventos extremos de crecidas. *Huellas* 23(1): 11–26. DOI 10.19137/huellas-2019-2302.

Wang X.L., Wen Q.H., Wu Y., 2007. Penalized maximal t test for detecting undocumented mean change in climate data series. *Journal of Applied Meteorology and Climatology* 46(6): 916–931. DOI 10.1175/2007JTECHA982.1.

Watanabe S., Kanae S., Seto S., 2012. Intercomparison of bias-correction methods for monthly temperature and precipitation simulated by multiple climate models. *Journal of Geophysical Research: Atmospheres* 117(D23): D23114. DOI 10.1029/2012JD018192.

Zhang Q., Li J., David Chen Y., 2011. Observed changes of temperature extremes during 1960-2005 in China: Natural or human-induced variations? *Theoretical and Applied Climatology* 106: 417–431. DOI 10.1007/s00704-011-0447-3.

Zhang X., Wan H., Zwiers F.W., Hegerl G.C., Min S.K., 2019. Attributing intensification of precipitation extremes to human influence. *Geophysical Research Letters* 46(4): 2325–2336. DOI 10.1002/grl.51010.

Zhang X., Yang F., 2004. *RClimDex (1.0) user manual*. Climate Research Branch Environment, Canada.

Zhou H., Aizen E., Aizen V., 2018. Constructing a long-term monthly climate data set in Central Asia. *International Journal of Climatology* 38(3): 1463–1475. DOI 10.1002/joc.5259.

Zilli M.T., Carvalho L.M., Lintner B.R., 2019. The poleward shift of South Atlantic convergence zone in recent decades. *Climate Dynamics* 52: 2545–2563. DOI 10.1007/s00382-018-4277-1.

Zscheischler J., Westra S., van den Hurk B.J.J.M., Seneviratne S.I., Ward P.J., Pitman A., AghaKouchak A., Bresch D.N., Leonard M., Wahl T., Zhang X., 2018. Future climate risk from compound events. *Nature Climate Change* 8: 469–896. DOI 10.1038/s41558-018-0156-3.